



**HAL**  
open science

## Surface sulphination of germanium oxide based materials

Laëtitia Petit, Kathleen Richardson, B. Campbell, Glenn Orveillon, Thierry Cardinal, François Guillen, Christine Labrugère, Philippe Vinatier, Michel Couzi, W. Li, et al.

► **To cite this version:**

Laëtitia Petit, Kathleen Richardson, B. Campbell, Glenn Orveillon, Thierry Cardinal, et al.. Surface sulphination of germanium oxide based materials. *Physics and Chemistry of Glasses - European Journal of Glass Science and Technology Part B*, 2004, 45 (6), pp.315-321. hal-00157926

**HAL Id: hal-00157926**

**<https://hal.science/hal-00157926>**

Submitted on 5 Feb 2024

**HAL** is a multi-disciplinary open access archive for the deposit and dissemination of scientific research documents, whether they are published or not. The documents may come from teaching and research institutions in France or abroad, or from public or private research centers.

L'archive ouverte pluridisciplinaire **HAL**, est destinée au dépôt et à la diffusion de documents scientifiques de niveau recherche, publiés ou non, émanant des établissements d'enseignement et de recherche français ou étrangers, des laboratoires publics ou privés.

# Surface sulphination of germanium oxide based materials

L. Petit<sup>1</sup>, K. Richardson<sup>a</sup>

Center for Research and Education in Optics and Lasers, College of Optics, University of Central Florida, 4000 Central Florida Boulevard, Orlando, FL32816, USA

B. Campbell, G. Orveillon, T. Cardinal, F. Guillen, C. Labrugere,  
P. Vinatier

Institut de Chimie de la Matière Condensée de Bordeaux (ICMCB), CNRS UPR 9048, Av. du Dr. A. Schweitzer, 33608 Pessac Cedex, France

M. Couzi

Laboratoire de Physico-Chimie Moléculaire (LPCM), CNRS UMR 5803, 351, cours de la Libération, 33405 Talence Cedex, France

W. Li & S. Seal

<sup>a</sup>AMPAC, Department of Mechanical, Materials and Aerospace Engineering, University of Central Florida, 4000 Central Florida Boulevard, Orlando, FL32816, USA

*The effect of oxygen substitution for sulphur has been investigated in germanium and boron based glasses containing heavy metal oxides ( $Sb_2O_3$ ). After heat treatment under  $H_2S$  flow, the colour of the glass (powder and bulk) changes from colourless to yellowish indicative of anion exchange. The oxygen substitution for sulphur has been confirmed by the presence of a new Raman band located at  $340\text{ cm}^{-1}$  corresponding to a Ge–S and Sb–S bond vibration. The influence of the borate addition has been studied. XPS measurements have shown (i) the oxidation of  $Sb^{3+}$  to  $Sb^{5+}$  during the melting which increases with an increase of boron content and (ii) the reduction of  $Sb^{5+}$  to  $Sb^{3+}$  during the sulphination, resulting in the departure of more than one oxygen anion upon replacement by one sulphur and in the absence of weight gain. It has been clearly demonstrated that sulphination near the oxide glass transition temperature can lead to the formation of oxysulphide glass materials.*

Chalcogenide glasses (ChG) have attracted the attention of many investigators due to the fact that they are potential candidates for applications in infrared optics and photonics device.<sup>(1–3)</sup> Their low optical band gap, high sensitivity to infrared and visible exposure, makes them good candidates for novel integrated optics. Grating fabrication or direct writing of waveguides has been demonstrated in ChG glasses using irradiation at 514

and 800 nm.<sup>(4–5)</sup> Nevertheless, at telecommunication wavelengths, photo-induced effects leading to structural modification often rule out their opportunities for use. To make the resulting materials more physically (thermally and mechanically) robust, further improvements to the glass composition must be made, so as to avoid material modification at 1500 nm. The proposed effort aims to identify suitably stable compositions, amenable to rare earth doping with minimal photosensitivity.

Sulphide materials have been identified as possible materials for nonlinear optical applications. Because of its large atomic radius compared to oxygen in oxide glasses, sulphur plays an important role in the nonlinear optical properties in sulphide glasses. It has been demonstrated that the substitution of oxygen anions by sulphur anions increases the  $\chi^{(3)}$  by one order of magnitude.<sup>(6)</sup> Additionally, oxysulphide, oxyhalide and chalcocalide glasses containing oxide and sulphide or halide components have been studied for optical application.<sup>(7)</sup> It has been reported that these glasses exhibit better chemical stability and are more resistant to atmospheric attack in comparison with the corresponding sulphide glasses though sometimes at the expense of a low glass transition temperature.<sup>(8)</sup> Such glass forming ability is also often better than pure oxides and chalcogenides.<sup>(9)</sup> Oxysulphide materials should offer the possibility of combining the attractive mechanical and chemical properties of oxide materials with the desirable optical traits of sulphide glasses by

<sup>1</sup> Corresponding author. Email: lpetit@mail.ucf.edu

modification of the sulphur to oxygen ratio.

Glasses in the  $\text{La}_2\text{O}_3$ – $\text{La}_2\text{S}_3$ – $\text{Ga}_2\text{S}_3$ – $\text{Ga}_2\text{O}_3$  system have been studied intensively over the last thirty years, for optical applications.<sup>(10)</sup> Good chemical and optical properties of these glasses were demonstrated. However, only a few studies involving antimony or germanium oxysulphide glass systems have been reported.<sup>(11)</sup> As antimony and germanium are considered good glass-formers, germanium oxide based glasses containing heavy metal oxides ( $\text{Sb}_2\text{O}_3$ ) have been studied for IR device applications.<sup>(12–13)</sup> Chalcogenides in similar glass systems ( $\text{Ge}$ – $\text{Sb}$ – $\text{S}$ ) show possible applications as optical transmission media.<sup>(14)</sup> A wide glass forming region has been observed, making property optimisation through compositional tailoring attractive. For these reasons, this work aims to develop oxysulphide glasses with good physical stability suitable for use in novel optical applications.

In this study, we present recent results of studies using heat treatment under  $\text{H}_2\text{S}$  gas flow of germanium based glasses for the preparation of oxysulphide materials. Micro-Raman spectroscopy and XPS have been conducted to verify the structural changes which occurred after the sulphination treatment. The influence of boron introduction into the system and its corresponding impact on glass properties have been, also, investigated.

## Experimental procedure

### Sample preparation

**Oxide glass synthesis** Germanium based glasses containing glass formers such as  $\text{B}_2\text{O}_3$  and  $\text{Sb}_2\text{O}_3$  have been elaborated. Glasses of the following composition  $(1-x)[0.71\text{GeO}_2-0.29\text{Sb}_2\text{O}_3].x\text{B}_2\text{O}_3$ , with  $x=0.06, 0.13$  and  $0.30$  have been prepared. The starting materials used were amorphous  $\text{GeO}_2$  (99.9%, Aldrich Chem. Co.),  $\text{Sb}_2\text{O}_3$  (99%, Aldrich Chem. Co.) and  $\text{H}_3\text{BO}_3$  (99.999%, Aldrich Chem. Co). Batch mixtures with the appropriate molar ratio of starting materials were subjected to a preliminary heat treatment to dry the starting materials and then melted in a platinum crucible for 15 min between 1100 and 1170°C depending on composition. The melt was then cast onto a stainless steel plate which had been preheated to 40°C below the glass transition temperature. After quenching, all oxide glasses were annealed for 15 h at 40°C below their glass transition temperature. The final germanium, antimony and boron content was confirmed to be identical to the initial batch concentrations introduced in the batch, by EDS (Elemental Dispersive Spectroscopy) with an accuracy of two atomic percent.

**Anion exchange** The substitution of oxygen by sulphur was carried out on oxide glass powder, which had been mechanically crushed into grains, yielding material with a grain size distribution between 1 and 100  $\mu\text{m}$ . The prepared powder and bulk specimens were treated in a furnace under  $\text{H}_2\text{S}$  flow, over 15 h, at 320°C. For all glasses examined, the treatment temperature was well below their glass transition temperature. EDS was used to monitor and evaluate the extent of sulphination and x-ray diffraction (XRD) was carried

out on each sample to confirm the post sulphination amorphous state of the treated powder.

### Property measurement

The glass transition ( $T_g$ ) and crystallisation ( $T_c$ ) temperatures of the untreated and treated glasses were determined by differential thermal analysis (DTA) at a heating rate of 10°C/min using a DSC apparatus (Seiko Instruments Inc.).

Density of bulk materials was measured by Archimedes' principle using diethylphtalate. The accuracy was better than 0.3%.

### Structural characterisation

The micro-Raman spectra were recorded with a Labram confocal micro-Raman instrument from Jobin-Yvon (typical resolution of about 2  $\text{cm}^{-1}$ ), in backscattering geometry at room temperature. The system consists of a holographic notch filter for Rayleigh rejection, a microscope equipped with 10 $\times$ , 50 $\times$  and 100 $\times$  objectives (the latter allowing a spatial resolution of less than 2  $\mu\text{m}$ ), and a CCD detector. The 632 nm emission line of a He–Ne laser was used for excitation with maximum incident power around 10 mW. The excitation power impinging on the sample during measurement was attenuated down to about 1 mW depending on the absorption of the sample.

### X-ray photoelectron spectroscopy

The pre- and post treatment surface chemistry of the samples were studied using a PHI-5400 x-ray photoelectron spectroscopy system at a vacuum of  $\sim 10^{-9}$  Torr. A non-monochromatic Mg  $K_\alpha$  x-ray source ( $h\nu=1253.6$  eV) at a power of 250 W was used for analysis. Survey spectra were recorded from 0 to 1100 eV with pass energy of 44.75 eV, using 0.5 eV steps and four scans. Individual high resolution spectra (C 1s, B 1s, Sb 3d, Ge 3d, Ge 2p and valence bands) were made with a pass energy of 35.75 eV, 0.05 eV steps, and scans numbering 20 to 50, depending on the intensity of the peak, to reach a satisfactory signal/noise ratio. Binding energies have been corrected using adventitious carbon (C 1s at 284.6 eV) as a reference.<sup>(15)</sup> Auger Scan software from RBD Enterprises was used to facilitate peak deconvolution.<sup>(16)</sup>

An x-ray photoelectron survey scan in the binding energy region 0–1200 eV was recorded for each glass sample. The low resolution XPS scan from the sulphinated powder of the glass with  $x=0.06$ , taken as an example, is shown in Figure 1. The core level peaks and x-ray induced Auger lines from the constituent elements are easily identified and marked on the spectrum.

## Results and discussion

The aim of this study was to investigate the effect of  $\text{H}_2\text{S}$  heat treatment on germanium based glasses and the influence of further boron introduction on the resulting glass properties. Raman spectroscopy and XPS have been conducted to evaluate the structural modification. The investigations have been focused on germanium and antimony environment. For both

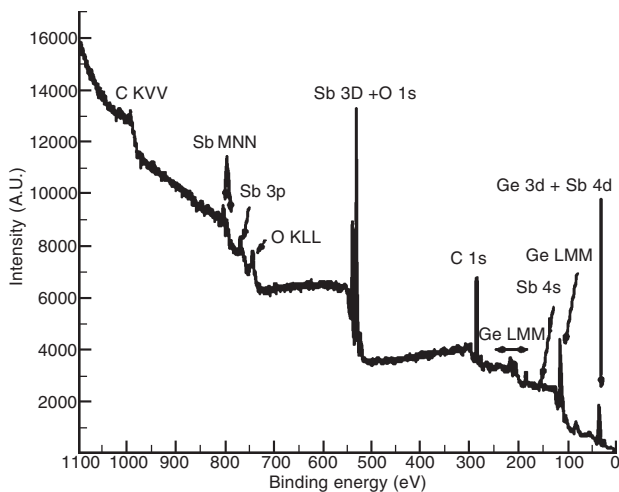


**Figure 1.** Low resolution XPS spectrum obtained from the glass with  $x=0.06$

techniques, no structural information directly related to borate units could be extracted due to the weakness of the signal associated to borate groups.

The glass transition temperature ( $T_g$ ) and the density ( $\rho$ ) of the investigated glasses prior to the sulphination heat treatment are reported in Table 1. When the concentration of  $B_2O_3$  increases, the  $T_g$  and the density decrease progressively. No evidence of a crystallisation temperature was measured up to a temperature of  $525^\circ C$ .

#### Structural results for germanium based oxide glasses

The normalised Raman spectra of the oxide glasses with varying Boron content ( $x$ ), measured prior to sulphination, are shown in Figure 2. The spectra exhibit a broad band at  $430\text{ cm}^{-1}$  and bands around  $700$  and  $800\text{ cm}^{-1}$ . When the concentration of  $B_2O_3$  increases, the broad band shifts to higher wavenumber and the intensity of the other bands in higher wavenumber can be easily distinguished for the larger amount of borate. According to previous Raman scattering investigations,<sup>(17–18)</sup> the Raman band observed at  $430\text{ cm}^{-1}$  has been assigned, not only, to Ge–O vibration but also to the asymmetric bending vibration modes of  $SbO_3$  pyramidal units. The Raman spectra of similar  $GeO_2$ – $B_2O_3$  glasses were investigated by Beys *et al.*<sup>(19)</sup> The band at  $720\text{ cm}^{-1}$ , seen only in this study at  $x=0.30$ , has been attributed to the formation of Ge–O–B bridges in which boron participates in boroxol groups. They attributed the band at  $808\text{ cm}^{-1}$  to these same boroxol groups. The relative intensity of the Ge–O–B band increases with  $B_2O_3$  content as expected and as seen in previous investigations, showing the establishment

**Table 1.** Germanium based oxide glasses composition  $(1-x)[0.71GeO_2-0.29Sb_2O_3]xB_2O_3$ , glass transition temperature and density before sulphination

Mo% $B_2O_3$ $x$	Glass transition temperature $T_g$ ( $^\circ C$ ) $\pm 5^\circ C$	Density $\rho$ ( $g/cm^3$ ) $\pm 0.02$
0.06	392	4.22
0.13	374	4.09
0.30	363	3.66

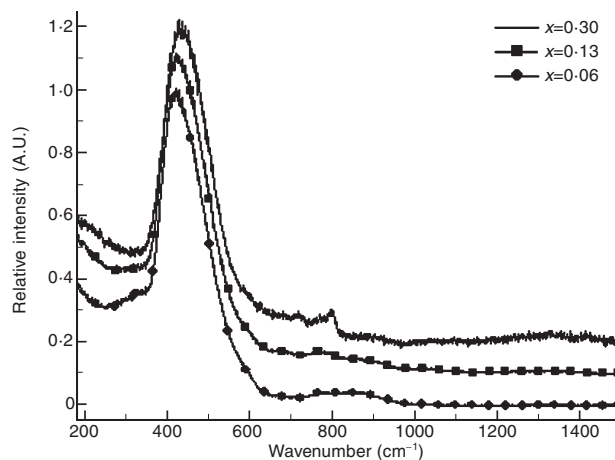


**Figure 2.** Micro-Raman spectra of oxide glasses versus the  $BO_3$  molar fraction  $x$  ( $\lambda_{exc}=632.8\text{nm}$ )

of the borogermanate glass network. The shift to higher wavenumber of the  $430\text{ cm}^{-1}$  band confirms the glass network modification with the progressive introduction of borate groups.

Figure 3(a) shows the fitted  $Sb\ 3d_{3/2}$  spectra of the investigated glasses with  $x=0.06$  and  $0.30$ . Only  $Sb\ 3d_{3/2}$  spectra were used for the peak deconvolution because of the overlapping of  $Sb\ 3d_{5/2}$  peak with  $O\ 1s$  peak. Two components,  $Sb_2O_3$  and  $Sb_2O_5$ , were needed to properly fit the spectra of the glasses. Their binding energies (BEs) were fixed at around  $539.14$  and  $539.94\text{ eV}$ , respectively. The binding energies were chosen based on our independent measurements on standard samples ( $Sb_2O_3$  and  $Sb_2O_5$ ) and confirmed by the referenced  $Sb\ 3d_{3/2}$  line in  $Sb_2O_3$ .<sup>(20)</sup> A peak separation of  $0.8\text{ eV}$  for the  $Sb\ 3d_{3/2}$  between  $Sb_2O_3$  and  $Sb_2O_5$  was fixed in the fitting procedure.<sup>(21)</sup> These peak binding energies and their widths did not show compositional variation. The relative fractions of Sb species in each of the two environments are given in Table 2. It has been noticed that the intensity of the peak corresponding to  $Sb^{5+}(O)$  increases slowly with an increase of  $B_2O_3$  content, indicating an increase of  $Sb_2O_5$  content with an increase of  $B_2O_3$ . In accordance with Pal *et al.*,<sup>(22)</sup> the presence of  $Sb^{5+}$  can be explained by the partial oxidation of  $Sb^{3+}$  during melting. The increase of the relative  $Sb^{5+}$  concentration with an increase of  $B_2O_3$  content indicates that borate groups in the glass network facilitate the oxidation of  $Sb^{3+}$  during the melting. A similar consistent variation in  $Sb^{5+}/Sb^{3+}$  content has been confirmed by the measurement of the  $Sb\ 4d$  spectra for both glasses with  $x=0.06$  and  $0.30$ , presented in the Figure 3(b). In these spectra, the  $Sb\ 4d$  peaks are overlapping with  $Ge\ 3d$  peaks. The  $Ge\ 3d$  photo-

**Table 2.** Ratios of the different  $Sb^{3+}$  and  $Sb^{5+}$  components in the fitted  $Sb\ 3d_{3/2}$  spectrum prior to and after sulphination treatment

Mo% $B_2O_3$ $x$	Relative fraction of each Sb species			
	Prior to sulphination $Sb^{3+}$ ( $Sb_2O_3$ )	$Sb^{5+}$ ( $Sb_2O_5$ )	After treatment $Sb^{3+}$ ( $Sb_2O_3$ )	$Sb^{5+}$ ( $Sb_2O_5$ )
0.06	60	40	6	5
0.30	48	52	8	25

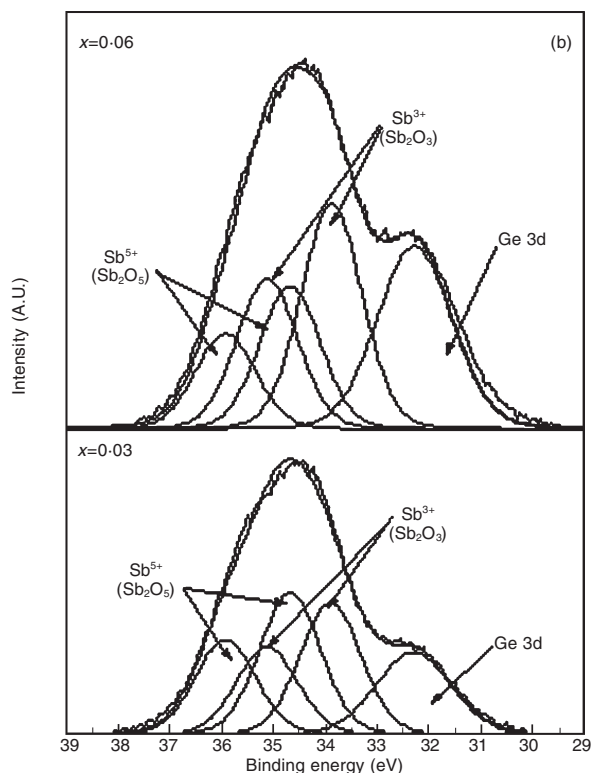
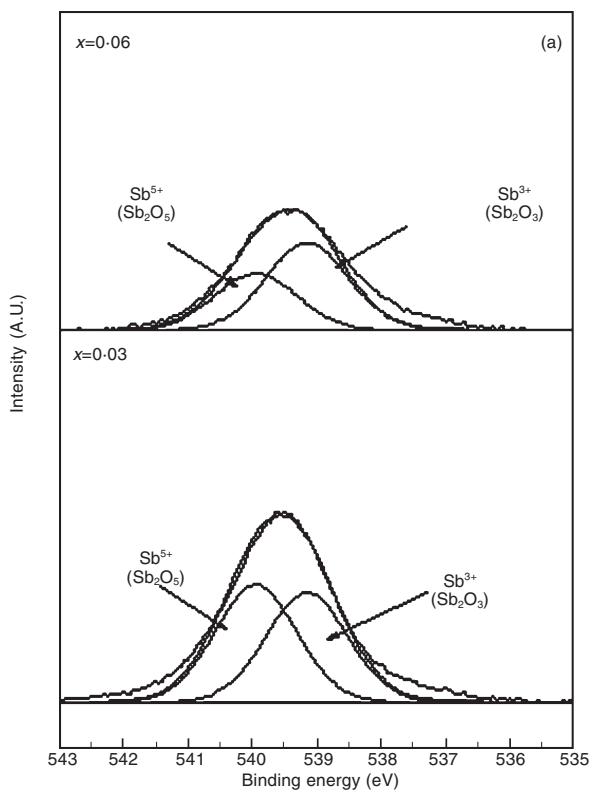


**Figure 3.** High resolution XPS spectrum of Sb  $3d_{3/2}$  (a) and of Ge (3d) and Sb (4d) levels (b) for the glasses in the system  $(1-x)[0.71\text{GeO}_2-0.29\text{Sb}_2\text{O}_3]x\text{B}_2\text{O}_3$  with  $x=0.06$  and  $0.30$  prior to sulphination treatment

electron peak binding energies and their widths did not show compositional variation.

#### Anion exchange: oxygen by sulphur

Germanium based glasses were heat treated under  $\text{H}_2\text{S}$  at  $320^\circ\text{C}$  for 15 h. Following the sulphination treatment, no weight gain of the powder nor the bulk samples was observed. The colour of the powder and bulk samples changed from colourless (white) to yellowish.

**Substitution of oxygen by sulphur in powder sample** X-ray diffraction (XRD) patterns, obtained on the post-treated powder, indicated no evidence of crystalline phase formation in the powdered glass.

The extent of anion exchange, oxygen for sulphur, was checked by measuring the micro-Raman spectrum of different grains of the powder after sulphination. Figure 4 shows spectra obtained from three different grains of post treated powder, indicating variability in the extent of anion exchange. As can be seen in Figure 4, the spectra of the sulphinated glass grains containing  $x=0.06$  show the same broad band, seen in glasses prior to treatment, around  $400\text{--}600\text{ cm}^{-1}$  and  $700\text{--}800\text{ cm}^{-1}$  confirming the presence of Ge–O and Sb–O bonds. Additionally, after sulphination, a new band appears between  $200$  and  $400\text{ cm}^{-1}$  peaking at  $345\text{ cm}^{-1}$ . This band can be attributed to Ge–S or Sb–S vibrations in accordance with Frumarova *et al.*<sup>(23)</sup> who assigned the band around  $280\text{--}310\text{ cm}^{-1}$  to the symmetrical vibration of the  $\text{SbS}_3$  pyramid and around  $330\text{--}340\text{ cm}^{-1}$  to the tetrahedral vibration of  $\text{GeS}_4$ . One can notice that the intensity of this band, in one of the recorded spec-

trum presented in Figure 4, has similar intensity as the broad band at  $400\text{--}600\text{ cm}^{-1}$ , showing that the sulphination heat treatment at this temperature can form an oxysulphide powder. The variation in the intensity of the band at  $280\text{--}310\text{ cm}^{-1}$  for the three grains examined however, demonstrates the inhomogeneous nature of the sulphination process when applied to glass powder. This effect should be related to the different grain sizes ( $1\text{--}100\text{ }\mu\text{m}$ ), which possess varying amounts of surface area available to the  $\text{H}_2\text{S}$  treatment.

Figure 5(a) illustrates the fitted XPS Sb  $3d_{3/2}$  spectra of the sulphinated glasses with  $x=0.06$  and  $0.30$ . These spectra have been fitted with three components attributed to  $\text{Sb}^{5+}$  in  $\text{Sb}_2\text{O}_5$ , and  $\text{Sb}^{3+}$  in  $\text{Sb}_2\text{O}_3$  and  $\text{Sb}_2\text{S}_3$ . A constant peak separation of  $0.5\text{ eV}$  for the Sb

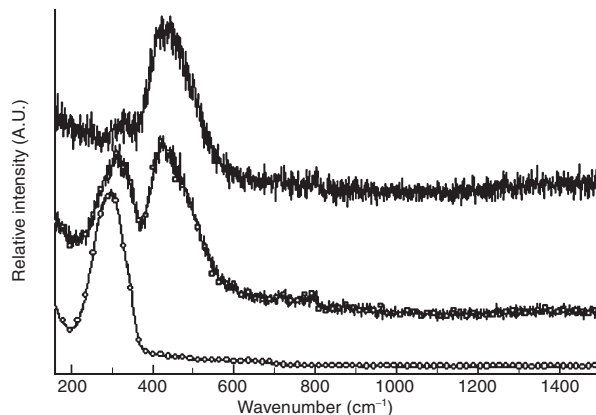


**Figure 4.** Micro-Raman spectra of the different sulphinated grains powder of the glass with  $x=0.06$  ( $\lambda_{\text{exc}}=632.8\text{ nm}$ )

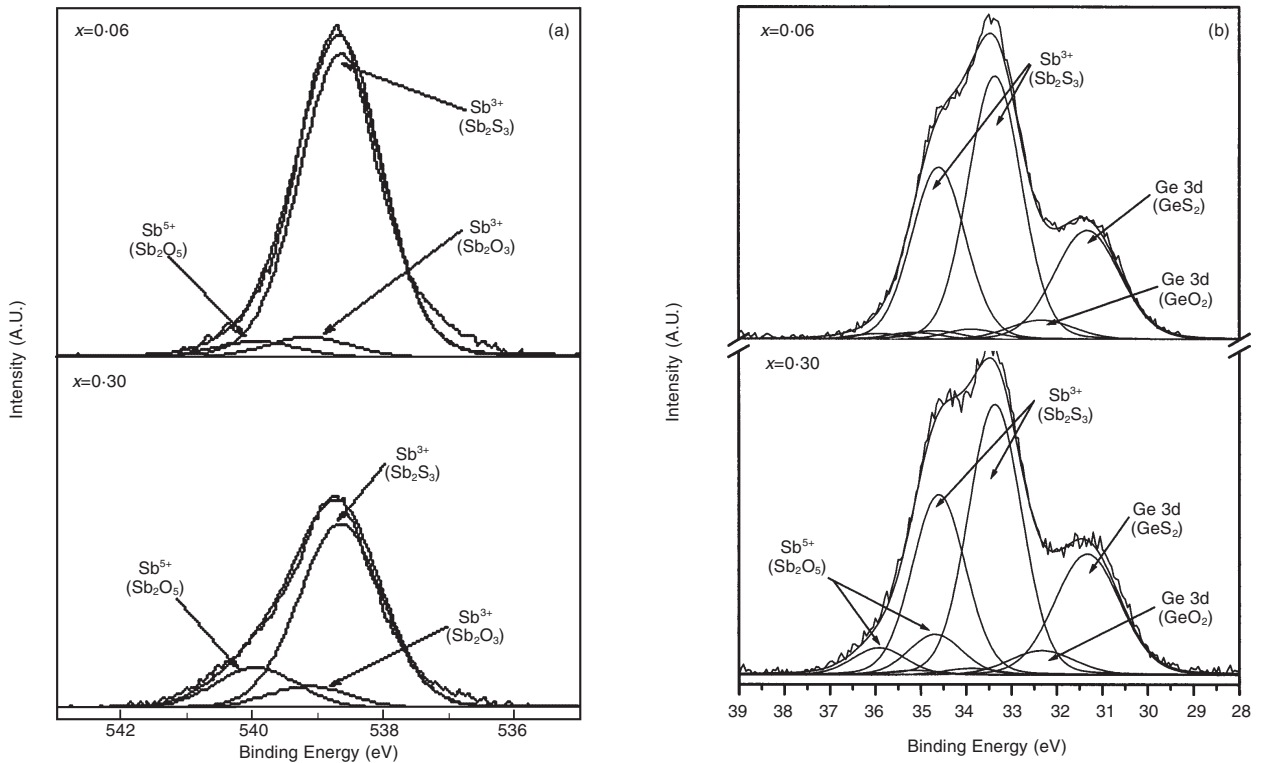


**Figure 5.** High resolution XPS spectrum of Sb ( $3d_{3/2}$ ) (a) and of Ge (3d) and Sb (4d) levels (b) from the glasses in the system  $(1-x)[0.71GeO_2-0.29Sb_2O_3]xB_2O_3$  after sulphination treatment

$3d_{3/2}$  between  $Sb_2O_3$  and  $Sb_2S_3$  was used in the fitting procedures to compare relatively the intensity of the XPS signal versus  $x$ . One can notice that the XPS signal of  $Sb^{3+}$  in  $Sb_2S_3$  is smaller in the spectrum of the glass with  $x=0.30$ , indicating a higher  $Sb^{5+}$  content in this glass. As presented in Table 2, the ratio  $Sb_2S_3/Sb_2O_5$  decreases strongly with the progressive introduction of borate groups indicating that the boron presence reduces the ease of anion substitution oxygen for sulphur around Sb in the glass. Moreover the ratio  $Sb_2O_5/Sb_2O_3$  increases dramatically for the largest borate concentration showing that the boron stabilises the  $Sb^{5+}$  against reduction. This phenomenon tends to suggest that borate groups are in the vicinity of the antimony units. The Sb 4d–Ge 3d spectra for the sulphinated glass with  $x=0.06$ , in Figure 5(b) taken as an example, has been deconvoluted into eight peaks. Compared to the non-sulphinated Sb 4d–Ge 3d fit, the doublet at 33.36–34.60 eV has been attributed to  $Sb_2S_3$  and the peak at 31.33 eV to  $GeS_2$ . The XPS data provide evidence that both  $GeO_2$  and  $GeS_2$  are present in the glass network after sulphination heat treatment. No noticeable variation of the ratio  $GeS_2/GeO_2$  has been measured with the progressive introduction of borate groups indicating no inhibition of sulphur replacement on Ge as seen for Sb with varying boron content.

The absence of measured weight gain after sulphination treatment can be explained by the reduction of  $Sb^{5+}$  ions to  $Sb^{3+}$ , resulting in the departure of more than one oxygen anion upon replacement by one sulphur, as one would mainly expect to find  $Sb^{3+}$  in sulphide glasses. Assuming this is the mechanism taking place in this experiment, considering the atomic weights

of oxygen and sulphur species, this may result in the lack of any observed weight variation.

The XPS experiments have further substantiated the anion exchange in Ge–O and Sb–O bonds during the sulphination heat treatment of glass powder. The presence of boron groups does not affect the efficiency of the anion substitution in Ge–O but does limit the substitution on Sb–O. No information on borate groups could be obtained in the study due to the weakness of the signals using Raman and XPS spectroscopy.

*Substitution of oxygen by sulphur in bulk glass samples* After sulphination heat treatment, no weight gain of the bulk glasses was measured up to the accuracy of the measurement ( $\pm 0.05\%$ ). The sulphination treatment has led to anion exchange on the surface of the bulk sample. The glasses exhibited higher density, providing further evidence of the anion exchange inferred by the change of the bulk glass colour. These results imply a contraction of the glass network with treatment. The density of the sulphinated bulk specimens increases with an increase in the content of  $B_2O_3$ . The density of the glass with  $x=0.06$  increases to  $(4.24 \pm 0.02)$  g/cm<sup>3</sup> after sulphination and of the glass with  $x=0.13$  to  $(4.14 \pm 0.02)$  g/cm<sup>3</sup>, an increase of 0.5 and 1.2%, respectively. Regarding the sulphination heat treatment temperature (320°C), the increase of the density has to be related to the increase of the  $T_g$  of the glass with an increase of  $x$ . The glass with  $x=0.13$  may exhibit at 320 °C a slightly lower viscosity (than  $x=0.06$ ) as it is closer to its glass transition temperature. Consequently, we can assume that there is better

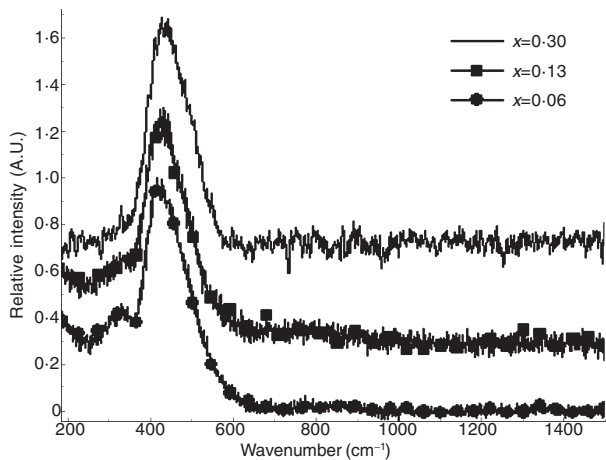


**Figure 6.** Micro-Raman spectra of sulphinated glasses versus the  $BO_3$  molar fraction  $x$  ( $\lambda_{exc} = 632.8 \text{ nm}$ )

diffusion of sulphur into the glass network when the sulphination treatment temperature is near to  $T_g$ .

Following sulphination, micro-Raman spectra were measured on the surface of the investigated bulk glasses. These spectra are illustrated in Figure 6. The spectra show broad bands around  $400\text{--}600 \text{ cm}^{-1}$ , as observed prior to sulphination, and a band at  $345 \text{ cm}^{-1}$  which has previously been observed in the micro-Raman spectra of the sulphinated powder samples. The spectra on different location on the surface of the sample were found to be identical, showing that the grain to grain variation observed in powder samples was not evident in bulk treatments. This band at  $345 \text{ cm}^{-1}$  has been attributed to Ge–S and Sb–S vibrations. One can notice that the intensity of this band decreases strongly with increasing  $B_2O_3$  content.

The glass with the lowest borate concentration ( $x=0.06$ ) which underwent the sulphination treatment temperature at  $320^\circ\text{C}$  (more than  $60^\circ\text{C}$  below its glass transition temperature) exhibits the highest sensitivity to anion exchange in Sb–O and/or Ge–O as its band at  $345 \text{ cm}^{-1}$  has the highest intensity. Accordingly, as shown in the XPS measurement in glass powder, this allows one to confirm that, similarly as in bulk glass,

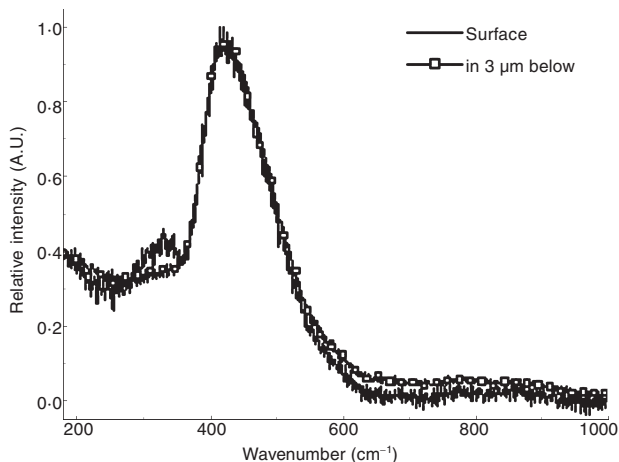


**Figure 7.** Micro-Raman spectra of glass composition  $(1-x)[0.71\text{GeO}_2-0.29\text{Sb}_2\text{O}_3]_x\text{B}_2\text{O}_3$  with  $x=0.06$  measured at the glass surface and below ( $\lambda_{exc}=632.8 \text{ nm}$ )

the borate groups seem to limit the anion exchange on Sb–O groups whereas no influence of borate groups on the anion exchange on Ge–O groups has been measured. Regarding these results, the increase of density variation after sulphination treatment with an increase of  $x$  may result from an increase of the anion exchange with B–O groups that we could not observe using XPS or Raman spectroscopy. Efforts to confirm this hypothesis are ongoing.

The post treatment surface of the glass with  $x=0.06$  can be considered an oxysulphide with a low anion exchange rate. To check the diffusion of sulphur across the sample, micro-Raman spectra were acquired at different depths in the glass. The micro-Raman spectra measured at the surface and at  $3 \mu\text{m}$  below are exhibited in Figure 7. One can see that the Raman band at  $345 \text{ cm}^{-1}$ , correlated to Ge–S and Sb–S, decreases with penetration depth showing the limited diffusion of S up to  $3 \mu\text{m}$  (the accuracy of the micro-Raman set up is  $1\text{--}2 \mu\text{m}$ ). The bulk glass appears to be oxysulphide in composition at the surface and predominantly oxide below this  $3 \mu\text{m}$  thick skin. The maximum diffusion depth possible under these treatment conditions has not been determined. The diffusion of the sulphur has to be quantified by Auger spectroscopy and this evaluation is ongoing.

## Conclusion

In this paper, we have demonstrated the successful production of stable oxide glass with an oxysulphide surface through the sulphination of germanium based oxide glasses at treatment temperatures near the glass transition temperature. Micro-Raman spectroscopy has been shown to be a powerful tool to monitor the extent of the sulphination of the oxide glass following  $\text{H}_2\text{S}$  treatment. Our Raman spectral investigations indicated that sulphination treatment performed on glass powder near the oxide glass transition temperature can lead to the formation of oxysulphide grains with varying levels of treatment uniformity. It has been shown that the anion exchange is not homogenous in the powder. In bulk glass samples, the sulphination treatment leads to an oxysulphide glass at the surface with a diffusion of sulphur inside the glass up to  $3 \mu\text{m}$ . The present study has demonstrated that germanium based glasses are suitable starting materials for oxysulphide glasses and anion exchange. The impact of such modification on other physical and optical properties is ongoing.

## Acknowledgments

The authors acknowledge the support of the National Science Foundation, International REU program (#EEC-9732420) whose support of this effort provided international research experiences to the undergraduates (BC) participating in this work. NSF grant # INT-0129235 supported the collaboration between the UCF and ICMCB groups through a joint NSF-CNRS program (No.13050). The author (KR) also acknowledges the support of NSF # DMR-9974129 that provided support during a sabbatical where this work was initiated.

## References

1. Nasu, H., Kubodera, R., Kobayasi, M., Nakamura, M. & Kamiya, K. *J. Am. Ceram. Soc.*, 1990, **73**, 1974.
2. Vogel, E. M., Weber, M. J. & Krol, D. M. *Phys. Chem. Glasses*, 1991, **32** (6), 231-54.
3. Nasu, H., Ibara, Y. & Kubodera, K. *J. Non-Cryst. Solids*, 1989, **110**, 229.
4. Viens, J. F., Meneghini, C., Villeneuve, A., Galstian, T. V., Knystautas, E. J., Duguay, M. A., Richardson, K. A. & Cardinal, T. J. *Lightwave Technol.*, 1999, **17** (7), 1184-91.
5. Meneghini, C. & Villeneuve, A. *J. Opt. Soc. Am. B*, 1998, **15** (12), 2946.
6. Zhou, Z. H., Nasu, H., Hashimoto, T. & Kamiya, K. *J. Mater. Res*, 1999, **14** (12), 330.
7. Lin, Z., Ling, H. & Cheng Shan Z. *J. Non Cryst. Solids*, 1995, **184**, 1.
8. Kumta, P. M. & Risbud, S. H., *Ceram Bull.*, 1990, **69**, 1977.
9. Zan, L., Zhong, J. & Luo, Q. *J. Non-Cryst. Solids*, 1999, **256-257**, 396-9.
10. Hwa, L. G., Shiau, J. G. & Szu, S. P. *J. Non-Cryst. Solids*, 1999, **249**, 55.
11. Riebling, E. F. *J. Mater. Sci.*, 1974, **9**, 753.
12. Nassau, K. & Chadwick, D. L. *Mater. Res. Bull.*, 1982, **17**, 715.
13. Nassau, K. & Chadwick, D. L., *J. Am. Ceram. Soc.*, 1982, **65**, 197.
14. Znobrik, A., Stetif, J., Kavich, I., Osipenko, V., Zachko, I., Balota, N. & Jakivchuk, O. *Ukr. Phys. J.*, 1981, **26**, 212.
15. Barr, T. L. & Seal, S., *J. Vac. Sci. Technol. A*, 1995, **13**, 1239.
16. RBD Enterprises, Inc., 563 Sw Bth St, Suite 201, Bend, OR 97702, USA.
17. Lines, C. *Opt. Commun.*, 1983, **4**, 2.
18. (a) Lines, M. E., Miller, A. E., Nassau, K. & Lyons, K. B. *J. Non-Cryst. Solids*, 1987, **89**, 163. (b) Terashima, K., Hashimoto, T., Uchino, T., Kim, S.-H. & Yoko, T. *J. Ceram. Soc. Jpn*, 1996, **104** (11), 1011-17.
19. Beys, L., Hillaire, P., Assih, T. & Phalippou, J. *J. Raman Spectrosc.*, 1983, **17**, 203.
20. Honma, T., Sato, R., Benino, Y., Komatsu, T. & Dimitrov, V. *J. Non-Cryst. Solids*, 2000, **272** (1), 1-13.
21. Delobel, R., Baussart, H., Leroy, J., Grimblot, J. & Gengembre, L. *J. Chem. Soc. Faraday Trans. I*, 1983, **79**, 879.
22. Pal, M. *J. Mater. Res.*, 1996, **11** (7), 1831.
23. Frumarova, B., Nemeč, P., Frumar, M., Oswald, J. & Vlček, M. *J. Non-Cryst. Solids*, 1999, **256-257**, 266.